

**BREAKTHROUGHS TAKE TIME.
ISOLATING CELLS SHOULDN'T.**



The Rheumatoid Arthritis Shared Epitope Triggers Innate Immune Signaling via Cell Surface Calreticulin

This information is current as of July 22, 2018.

Song Ling, Xiujun Pi and Joseph Holoshitz

J Immunol 2007; 179:6359-6367; ;
doi: 10.4049/jimmunol.179.9.6359
<http://www.jimmunol.org/content/179/9/6359>

References This article **cites 51 articles**, 10 of which you can access for free at:
<http://www.jimmunol.org/content/179/9/6359.full#ref-list-1>

Why *The JI*? [Submit online.](#)

- **Rapid Reviews! 30 days*** from submission to initial decision
- **No Triage!** Every submission reviewed by practicing scientists
- **Fast Publication!** 4 weeks from acceptance to publication

**average*

Subscription Information about subscribing to *The Journal of Immunology* is online at:
<http://jimmunol.org/subscription>

Permissions Submit copyright permission requests at:
<http://www.aai.org/About/Publications/JI/copyright.html>

Email Alerts Receive free email-alerts when new articles cite this article. Sign up at:
<http://jimmunol.org/alerts>

The Journal of Immunology is published twice each month by
The American Association of Immunologists, Inc.,
1451 Rockville Pike, Suite 650, Rockville, MD 20852
Copyright © 2007 by The American Association of
Immunologists All rights reserved.
Print ISSN: 0022-1767 Online ISSN: 1550-6606.



The Rheumatoid Arthritis Shared Epitope Triggers Innate Immune Signaling via Cell Surface Calreticulin¹

Song Ling, Xiujun Pi, and Joseph Holoshitz²

The shared epitope (SE), carried by the vast majority of rheumatoid arthritis patients, is a 5-aa sequence motif in the third allelic hypervariable region of the HLA-DR β chain. We have recently demonstrated that the SE acts as an allele-specific ligand that triggers NO-mediated pro-oxidative signaling in opposite cells. The identity of the cell surface molecule that interacts with the SE is unknown. Using affinity chromatography purification, cell-binding assays, surface plasmon resonance, and time-resolved fluorescence resonance energy transfer techniques, we have identified cell surface calreticulin (CRT) as the SE-binding molecule. SE-triggered signaling could be blocked by anti-CRT Abs or Abs against CD91 and by CRT-specific antisense or small-interfering RNA oligonucleotides. Embryonic fibroblasts from *crt*^{-/-} or CD91-deficient mice failed to transduce SE-triggered signals. Exogenously added soluble CRT attached to the cell surface and restored SE-triggered signaling responsiveness in *crt*^{-/-} cells. These data indicate that cell surface CRT, a known innate immunity receptor, which has been previously proposed as a culprit in autoimmunity, plays a critical role in SE-triggered signal transduction. *The Journal of Immunology*, 2007, 179: 6359–6367.

Genetic associations with particular class I or class II MHC alleles have been noticed in many autoimmune diseases. Based on the known role of MHC molecules in thymic selection and Ag presentation, it has been postulated that the mechanism underlying these associations involves T cell repertoire selection and/or presentation of self-Ags. Evidence to support this paradigm exists in some diseases, but in other cases, the basis for MHC-disease association remains unclear. For example, over 90% of rheumatoid arthritis (RA)³ patients carry *HLA-DRB1* alleles, which encode a 5-aa sequence motif, known as the shared epitope (SE), in position 70–74 in the β 1 domain of the HLA-DR molecule (1). The mechanistic basis of SE-RA association is presently unknown.

Class II MHC and classical class I MHC molecules are adaptive immune system glycoproteins, which specialize in Ag presentation to T cells carrying the CD4 or CD8 surface markers, respectively. In addition to their ability to present antigenic peptides, class I MHC molecules can trigger innate immunity signals through a pair of ligands located, respectively, in the α 1 and α 2 domains of the class I molecule (2). The α 2 domain of the class I MHC superfamily is of particular interest, because it contains ligands, which interact with a diverse repertoire of inhibitory or activating innate

immunity receptors, such as killer Ig-like receptors (KIR), the NKG2/CD94 heterodimeric receptor, and the NKG2D receptor (2–4). Moreover, this domain has been found to contain ligands for nonimmune system receptors, such as transferrin receptor (5) or the V2R pheromone receptor (6). Thus, the class I MHC α 2 domain appears to have preserved throughout evolution an ability to interact with a wide range of receptors mediating diverse biological functions.

It is noteworthy that x-ray crystallography studies have demonstrated that despite their functional divergence through evolution, the β 1 domain of the class II HLA-DR molecule and the α 2 domain of the class I HLA molecule have a remarkably similar tridimensional structure (7). It is therefore intriguing that the SE, located in the HLA-DR β 1 domain, is capable of triggering innate signaling in opposite cells (8, 9), reminiscent of innate immune signaling triggered by class I α 2 domain ligands (reviewed in Ref. 10).

In previous studies, we have found that the SE acts as a ligand that activates NO-mediated pro-oxidative signaling in opposite cells (8, 9). For example, cells carrying SE-positive *HLA-DRB1* alleles displayed increased constitutive NO production, which resulted in higher levels of reactive oxygen species and higher susceptibility to oxidative DNA damage. The signaling aberration could be transferred to SE-negative cells by cDNA transfection, indicating that SE-associated signaling activity is not due to linkage disequilibrium with another gene. Importantly, recombinant proteins, HLA-DR tetramers, and short synthetic peptides containing the SE motif could all mimic the signaling effect of the native SE-positive DR molecule.

To better understand the mechanisms involved in SE-triggered signaling, in this study, we have undertaken to identify the SE-binding receptor. Using peptide affinity chromatography, N-terminal amino acid sequencing, surface plasmon resonance (SPR), time-resolved fluorescence resonance energy transfer (TR-FRET), and cell-binding assays, we have determined that cell surface calreticulin (CRT) is a SE-binding molecule. The involvement of CRT in SE-triggered signaling was confirmed by demonstrating an inhibitory effect with anti-CRT Abs and with CRT-targeted antisense or small-interfering RNA

Department of Internal Medicine, University of Michigan, Ann Arbor, MI 48109

Received for publication June 14, 2007. Accepted for publication August 22, 2007.

The costs of publication of this article were defrayed in part by the payment of page charges. This article must therefore be hereby marked *advertisement* in accordance with 18 U.S.C. Section 1734 solely to indicate this fact.

¹ J.H. was supported by grants from the National Institutes of Health (AI47331, AR46468, AR20557, and AR48310) and by Basic Research Grants from the Arthritis Foundation and the American College of Rheumatology. X.P. was supported by Postdoctoral Training Grant AR07080 from the National Institutes of Health.

² Address correspondence and reprint requests to Dr. Joseph Holoshitz, University of Michigan, 5520D Medical Science Research Building 1, 1150 West Medical Center Drive, Ann Arbor, MI 48109-0680. E-mail address: jholo@umich.edu

³ Abbreviations used in this paper: RA, rheumatoid arthritis; SE, shared epitope; SPR, surface plasmon resonance; TR-FRET, time-resolved fluorescence resonance energy transfer; CRT, calreticulin; siRNA, small-interfering RNA; HSP, heat shock protein; MEF, murine embryonic fibroblast; RU, resonance unit.

Copyright © 2007 by The American Association of Immunologists, Inc. 0022-1767/07/\$2.00

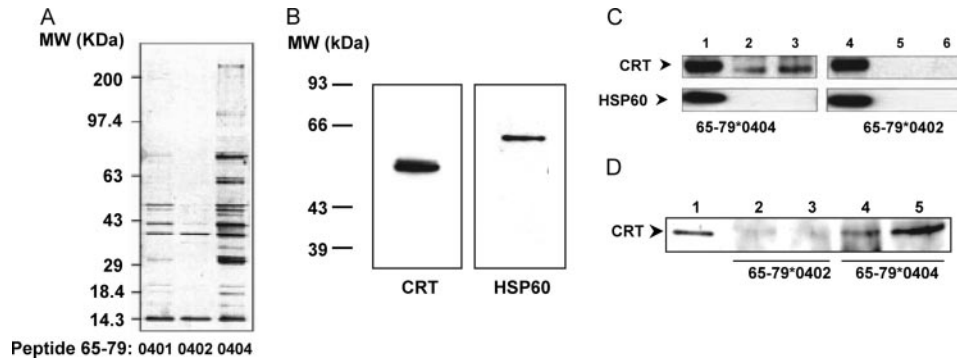


FIGURE 1. Purification and identification of SE-binding proteins. *A*, The following synthetic 15-mer peptides were immobilized on Sepharose beads and packed in the affinity columns: 65–79*0401 (*left*); 65–79*0402 (*center*); 65–79*0404 (*right*). M1 cells were lysed and protein extracts were loaded onto peptide affinity columns. Following extensive washing, bound proteins were eluted, separated on SDS-PAGE, and silver stained. *B*, To verify the identity of bands number 9 and 11 (Table I), eluates from peptide 65–79*0404 affinity columns were immunoblotted with either 1/1000-diluted anti-human CRT (*left*), or 1/2000-diluted ML-30 anti-human HSP60 (*right*). *C*, Purified recombinant rabbit CRT (*upper panel*) or human HSP60 (*lower panel*) were loaded onto peptide affinity columns carrying either the SE-positive 15-mer peptide, 65–79*0404 (*lanes 1–3*), or a SE-negative peptide 65–79*0402 (*lanes 4–6*). Following washings and elution, the different fractions were run on a SDS-PAGE, transferred to polyvinylidene difluoride membrane and blotted with anti-CRT or anti-HSP60 as above. *Lanes 1* and *4* represent effluents obtained during the loading process; *lanes 2* and *5* show eluates at pH 4.0; *lanes 3* and *6* show eluates at pH 2.0. *D*, Cell surface proteins were biotinylated, purified on a monomeric avidin affinity column, and then subjected to affinity chromatography on columns prepared with SE-negative 15-mer peptide 65–79*0402 (*lanes 2* and *3*) or with the SE-positive peptide 65–79*0404 (*lanes 4* and *5*). The different fractions were then run on SDS-PAGE and immunoblotted with anti-CRT Abs as above. *Lanes 2* and *4* show eluates at pH 4.0; *lanes 3* and *5* show eluates at pH 2.0. *Lane 1* represents a positive control (rCRT).

(siRNA) oligonucleotide transfection. Embryonic fibroblasts from CRT-deficient mice were unable to respond to the SE ligand, but regained signaling activity when CRT was added back to the cell culture.

Materials and Methods

Reagents and cells

rCRT and its truncated N-terminal domain were purified as previously described (11). Recombinant human heat shock protein (HSP) 60 was donated by Dr. H. Gaston (University of Cambridge, Cambridge, U.K.). All recombinant proteins were used at over 90% purity. Rabbit anti-CRT polyclonal Ab PA3–900 was purchased from Affinity Bio Reagents. The mouse anti-human HSP60 mAb ML-30 was a gift from Dr. J. Ivanyi (King's College, London, U.K.). Cy5-labeled streptavidin was purchased from Amersham Biosciences and monoclonal anti-GST Ab labeled with europium cryptate was from CIS Bio-International. Peptides were synthesized, purified, and immobilized on activated Sepharose as we previously described (8, 9). Human and mouse fibroblast lines were maintained in culture as we previously described (8). Murine embryonic fibroblasts (MEF) from wild-type (K41) and *crt*^{-/-} (K42) mice were generated as described (12) and donated by Dr. M. Michalak (University of Alberta, Edmonton, Canada). The CD91-deficient PEA-13 MEF line was purchased from American Type Culture Collection. All other reagents were purchased from Sigma-Aldrich.

Peptide affinity chromatography

Three-milliliter affinity matrices were packed into Bio-Rad PolyPrep columns. Columns were washed with 16 ml each of the following wash buffers: 0.1 M NaHCO₃, 0.5 M NaCl (pH 8.0), then 0.5 M CH₃COONa (pH 4.0) and, finally, with PBS (Ca²⁺ and Mg²⁺ free) at pH 7.5. M1 cell suspensions were washed with PBS and resuspended in 750 μ l of lysis buffer. Cells were passed 12 times through a 26-G needle using a 3-ml syringe. Cell lysates were kept on ice for 20 min and subsequently microcentrifuged at 15,000 rpm for 30 min in 4°C. Supernatants were loaded, 0.7 ml onto each column. Columns were incubated overnight in 4°C with gentle rotation. At the end of incubation, columns were washed with 32 ml of pre-elution buffer in 4°C and transferred to room temperature to equilibrate. Bound proteins were eluted successively with 20 mM glycine buffer as follows: 10 ml of glycine at pH 4.0, then, 6 ml of at pH 3.0, and finally 6 ml at pH 2.0. Protein concentration was determined by the Pierce Coomassie Plus assay at wavelength 595. The eluates were concentrated with Centricon 10 filters. Fifteen microliters per lane were loaded onto NuPage 4–12% gradient MOPS gels, using a standard protocol recommended by the manufacturer (Invitrogen Life Technologies). Proteins were transferred to polyvinylidene difluoride membranes, stained with Coomassie and processed for sequencing by the University of Michigan Protein Structure Facility, or directly stained with the Bio-Rad Silver Stain Plus kit, following the manufacturer's instructions.

Table I. N-terminal amino acid sequencing

Band No.	Molecular Mass (kDa)	Sequence ^a	Homology (Swissprot Accession Number)	Codon No.
1	18	PEPAKSAPAP	Human histone H2B.1 (Q93080)	2–11
2	22	DEKKKGPVKVT	Human cyclophilin B precursor (P23284)	26–35
3	27	LHTDGDKAFV	Human Pre-mRNA splicing factor SF2, P32 subunit/GC1q-R protein (Q07021)	74–83
4	29	GKGDPNKPRG	Human HMG-2 (P26583)	2–11
5	31	KGDPKKPRG	Human HMG-1 (P09426)	3–11
6	38	FVKVKKNKAYFKRY ^b	Human 60S ribosomal protein L5 (P46777)	3–16
7	39	GKVKVGVNGF	Human GAPDH (P04406)	2–11
8	42	PYQYPALTPPE	Human fructose-bisphosphate aldolase A (P04075)	2–11
9	50	EPAVYFKEQF	Human calreticulin precursor (P27797)	18–27
10	53	DAPEEEDHVL	Human protein disulfide isomerase precursor (P07237)	18–27
11	58	AKDVKFGADA	Human 60-kDa heat shock protein precursor, HSP60 (P10809)	27–36

^a In single letter form.

^b "X", Unsuccessful determination of amino acid identity.

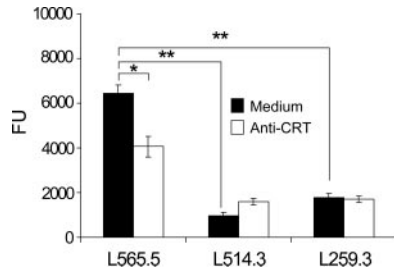


FIGURE 2. Interaction between native cell surface CRT and SE-positive HLA-DR molecules. M1 cells were labeled with a fluorescent vital dye 5-chloromethylfluorescein diacetate and added to monolayers of L cell transfectants expressing either *DRB1*0401* (L565.5), **0402* (L514.3), or **0403* (L259.3) and allowed to form cell-cell contact in the presence (□) or absence (■) of anti-CRT Abs. At the end of incubation, cultures were washed with PBS and fluorescence signals in individual wells were quantified. *, $p < 0.005$; **, $p < 10^{-5}$.

Biotinylation of cell surface proteins

M1 cells were incubated with 0.5 mg/ml EZ-Link Sulfo-NHS-LC-Biotin (Pierce) for 10 min at 37°C. The reaction was terminated by adding Tris-HCl (pH 7.5) at a final concentration of 50 mM. Cells were then washed in PBS, centrifuged, and solubilized in PBS containing 2% Nonidet P-40, followed by a brief sonication. Biotinylated proteins were purified on ImmunoPure-immobilized monomeric avidin columns (Pierce) using the protocol provided by the manufacturer. The bound biotinylated proteins were eluted from the column with 5 mM D-biotin in PBS containing 1% Nonidet P-40. The eluted proteins were concentrated on Centricon YM-3 columns (Millipore) before being subjected to peptide affinity chromatography.

Oligonucleotide transfection

CRT sense and antisense phosphorothioate oligonucleotides were synthesized by Operon Technologies: antisense, 5'-GGATAGCAGCATGGCGG GCCC-3'; sense, 5'-CGGCCCGCCATGCTGTATCC-3'.

M1 cells were cultured in 6-well plates to 60–70% confluence and treated with 0.2 μM oligonucleotide, using lipofectin as a carrier. Cells

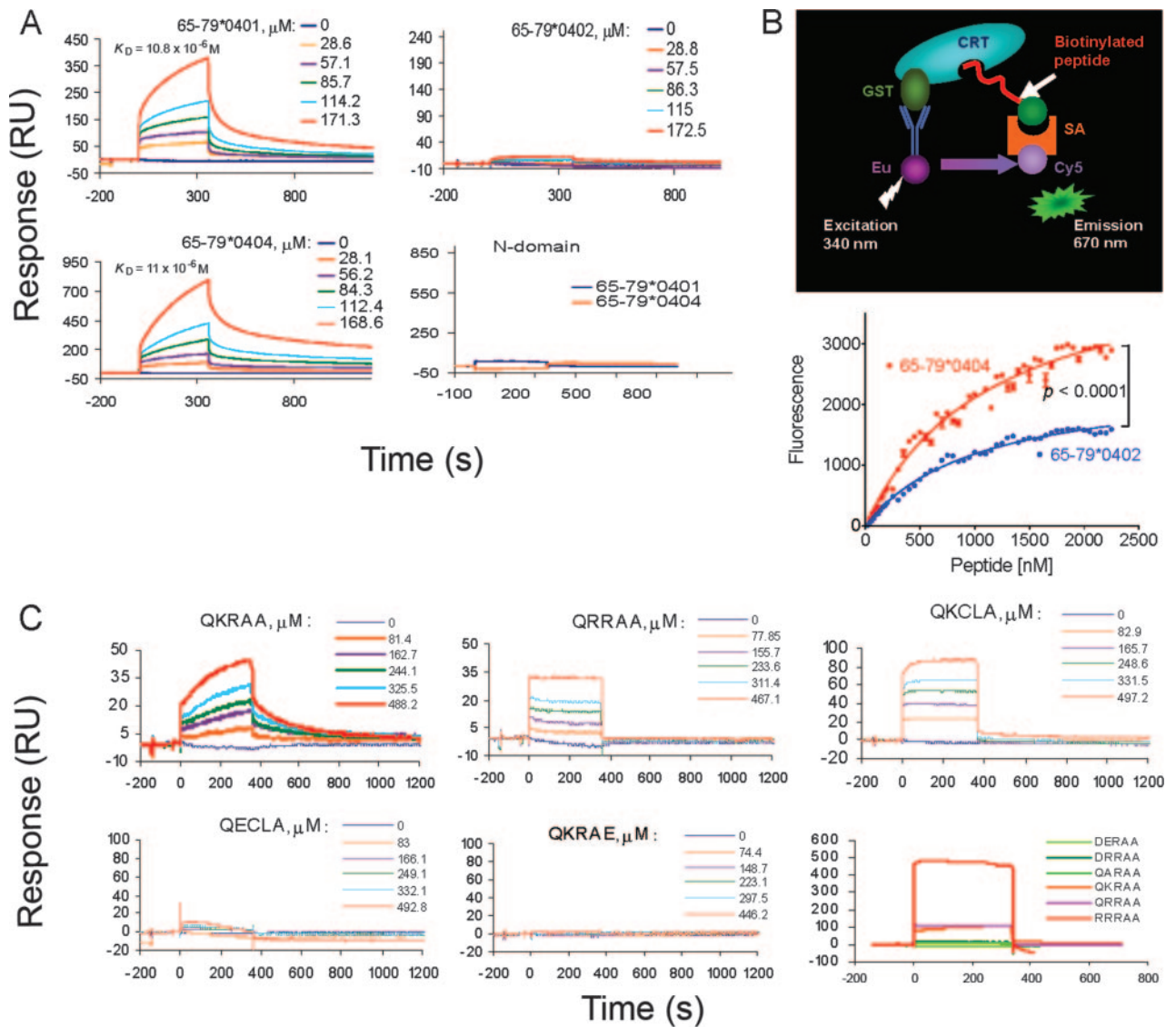
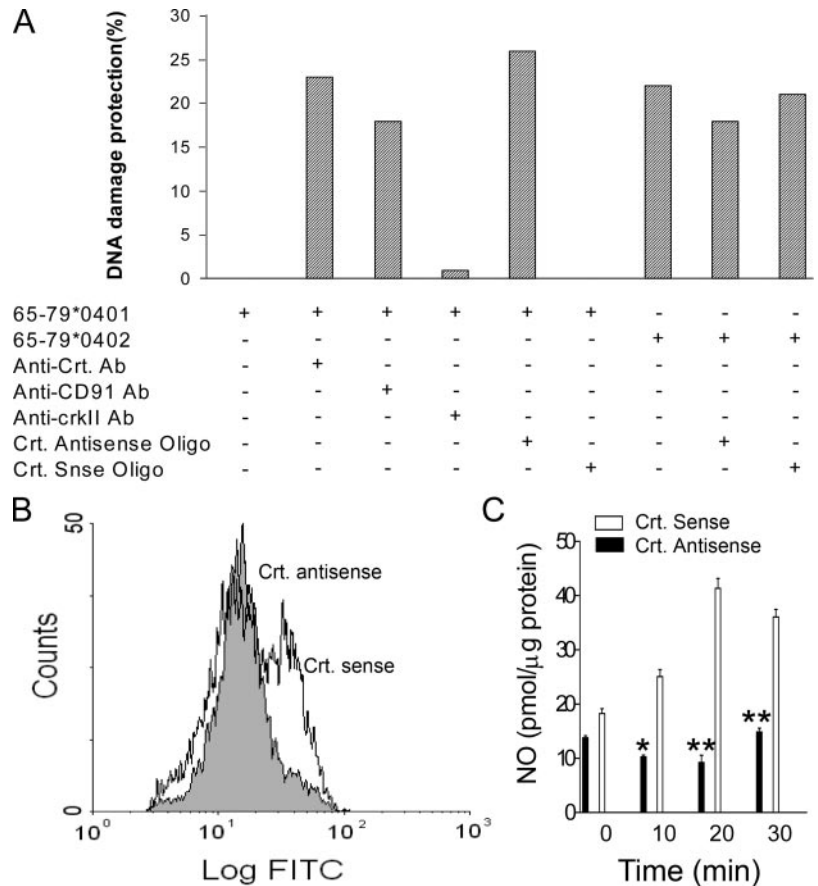


FIGURE 3. A, Representative sensorgrams derived from injection of different concentrations of 15-mer peptides over chip-immobilized CRT. Kinetic data were calculated using a monovalent ligand model. Sensorgrams with peptides 65–79*0401 (upper left), 65–79*0402 (upper right), and 65–79*0404 (lower left) are shown. In addition, truncated CRT mutant containing the N-domain only was immobilized on a different CM5 biosensor chip and used as a protein control (lower right). Fifteen-mer peptides, 65–79*0401 or 65–79*0404, were injected in the analyte. B, TR-FRET analysis of 15-mer peptide interaction with CRT. Upper panel, Schematic diagram of a TR-FRET-based CRT/SE-binding assay. Energy transfer from the donor to the acceptor is only possible when the distance is $< 100 \text{ \AA}$. SA, Streptavidin; Eu, europium cryptate. Lower panel, FRET is shown as the ratio of fluorescence in 665/620 nm wavelengths $\times 10^4$. Measurements were done in quadruplet wells and the values represent mean \pm SD. C, SPR analysis of 5-mer peptide interaction with CRT. Representative sensorgrams derived from injection of different concentrations of peptides over immobilized CRT.

FIGURE 4. A, Anti-CRT Abs and CRT antisense oligonucleotides inhibit SE signaling. M1 cells were preincubated for 30 min with a 1/500 dilution of rabbit anti-human CRT, or control rabbit anti-Crk II Abs. Other M1 cells were transfected with either CRT antisense oligonucleotides, or with sense CRT oligonucleotides. At the end of incubation, all cells were washed and incubated overnight with either the SE-positive 15-mer peptide, 65–79*0401, or with the SE-negative 15-mer control peptide, 65–79*0402, each at 50 $\mu\text{g}/\text{ml}$. Cells were then incubated with 10 μM 2-chloroadenosine for 20 min and subsequently subjected to oxidative stress with 100 μM H_2O_2 . The extent of DNA damage was determined as described (9). B, CRT antisense oligonucleotides suppress CRT surface expression. M1 cells were incubated with CRT antisense oligonucleotides (shaded histogram), or CRT sense oligonucleotides (white histogram). At the end of incubation, cells were washed and stained with rabbit anti-human CRT Abs and analyzed by flow cytometry. C, CRT antisense oligonucleotides block SE-triggered NO. M1 cells transfected with CRT antisense oligonucleotides, or CRT sense oligonucleotides as above were incubated for various times with Sepharose-immobilized 65–79*0401 peptide. NO levels were determined at various time points. *, $p < 0.005$; **, $p < 0.001$.



were cultured in medium for 48–96 h before experiments were performed. For siRNA experiments, a *crt*-targeted 21-nt (5'-AAGAAGA TAAAGGACCCTGAT-3') was designed using the Qiagen siRNA software. A scrambled 21-nt siRNA was used for control (Qiagen). Briefly, 10^7 L cells were transfected with an Amaxa nucleofector apparatus. After transfection, cells were cultured for 48–96 h before analyzing gene-silencing effects. Levels of mRNA were measured by quantitative real-time RT-PCR using TaqMan probes. CRT transcription levels were normalized to the housekeeping control gene hydroxymethylbilane synthase (HMBS).

Surface plasmon resonance

A Biacore2000 Biosensor System (Pharmacia/LKB Biotechnology) was used to assay the interaction of soluble synthetic peptides with rCRT. A SPR assay is based on a biosensor chip with a dextran-coated gold surface that is coated with a covalently immobilized protein. Binding of an injected ligand (the “analyte”) to the immobilized protein results in changes of the SPR that are directly proportional to the amount of bound ligand. Results are read in real time as resonance units (RU).

Before use, biosensor chips CM5 (Biacore) were preconditioned in water at 100 $\mu\text{l}/\text{min}$ by applying two consecutive 20- μl pulses of 50 mM NaOH, followed by 10 mM HCl, and finally 0.1% SDS. CM5 surface was activated by a 7-min injection of 200 mM 1-ethyl-3-(3-dimethylamino-propyl) carbodiimide hydrochloride in 50 mM *N*-hydroxysuccinimide. Purified CRT or its truncated N domain was immobilized by standard primary amines coupling in 25°C in HBS-EP buffer (10 mM HEPES (pH 7.4), 150 mM NaCl, 1 mM EDTA, and 0.005% surfactant P-20), at a flow rate of 10 $\mu\text{l}/\text{min}$. The protein was injected manually at a rate of 100 $\mu\text{g}/\text{ml}$ until approaching 5500 RU. The remaining activated groups were blocked by ethanolamine (1 M).

Binding assays were performed at 25°C in a binding buffer (10 mM HEPES (pH 7.4), 50 mM KCl, 0.5 mM CaCl_2 , 100 μM ZnCl_2 , and 0.005% surfactant P-20) at a flow rate of 10 $\mu\text{l}/\text{min}$. Peptides were in the analyte at different concentrations, ranging from 0 to 500 μM . Each experiment was repeated at least three times. The binding data were analyzed using the BIAevaluation version 3.0.1 program (Biacore).

TR-FRET

Biotin-labeled peptides were synthesized by Bioworld. All experiments were performed in an assay buffer of 25 mM HEPES (pH 7.7), 20 mM KCl, 0.5 mM CaCl_2 , and 0.1% BSA. Experiments were conducted in ProxiPlate 384-well microtiter plates (PerkinElmer) in 25- μl volumes. Five microliters of monoclonal anti-GST Ab labeled with europium cryptate in assay buffer was added to a mixture of 10 μl of 100 nM GST-CRT fusion protein and 5 μl of biotin-labeled peptide at different concentrations. After 1 h of incubation, 5 μl of 150 nM Cy5-labeled streptavidin were added and the plates were incubated overnight at 4°C. Energy transfer was measured by exciting at 340 nm and monitoring the emission for 50 μs at 670 nm, using a Fusion αHT Universal Microplate Analyzer (PerkinElmer Life Sciences) configured for time-resolved fluorescence after a 400 μs delay.

Cell-binding assays

L cell transfectants were incubated overnight in a 96-well plate (6×10^4 cells/well). M1 cells were labeled with 5-chloromethylfluorescein diacetate (Molecular Probes/Invitrogen Life Technologies). Labeled cells were incubated with or without anti-CRT Ab at a 1/100 dilution for 45 min. M1 cells were added at 2×10^4 /well to the L cell monolayers and allowed to bind to the L cells during a 15-min culture at 37°C. Wells were then washed three times with PBS to remove nonbinding cells and the remaining cells were fixed with 10% formalin. Plates were then read at 485-nm excitation filter and 535-nm emission wavelengths, using a Fusion αHT system (PerkinElmer Life Sciences).

Signal transduction assays

NO concentrations and production rates and pro-oxidative signaling were determined as we previously described (8, 9).

Results

As a first step to identifying candidate SE-binding molecules, M1 cell protein extracts were loaded onto peptide affinity columns prepared with synthetic peptides corresponding to the region 65–79

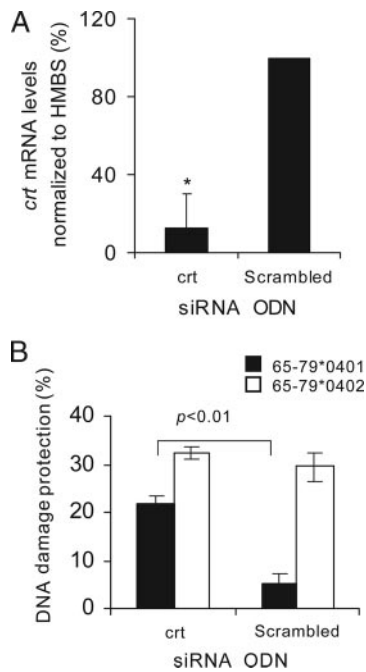


FIGURE 5. CRT-targeted gene knockdown experiments. *A*, L cells were transfected with either CRT-specific or scrambled siRNA oligonucleotides and mRNA expression levels, relative to mRNA expression of the housekeeping gene *HMBS*, were determined by real-time RT-PCR. *B*, L cells were transfected with either CRT-specific or scrambled siRNA oligonucleotides and subsequently incubated overnight with 100 $\mu\text{g/ml}$ SE-positive peptide 65–79*0401, or SE-negative peptide 65–79*0402. At the end of incubation, susceptibility of treated cells to DNA damage was determined as in Fig. 4.

encoded by SE-positive and -negative *HLA-DRB1* alleles. As can be seen (Fig. 1*A*), the eluates from affinity columns prepared with SE-positive peptides (65–79*0401 or 65–79*0404) displayed multiple protein bands. In contrast, the eluates from column prepared with a SE-negative peptide (65–79*0402) contained a single band (~39 kDa), which appeared to bind nonspecifically to all three columns.

The N termini of 11 protein bands were successfully sequenced (Table I). Of these, two are of special interest: CRT and HSP60, as both of them are found on the cell surface (13, 14) and have been previously implicated in the pathogenesis of RA (15, 16). The identities of these two bands as CRT and HSP60 were confirmed by immunoblotting (Fig. 1*B*). Because both HSP60 and CRT are chaperones, we reasoned that their retention on the affinity column could have been due to either direct binding to the SE peptide, or indirect association via another protein. To address this question, we loaded purified rCRT or HSP60 onto peptide affinity columns. As can be seen (Fig. 1*C*), CRT bound to the SE-positive peptide 65–79*0404 affinity column, while HSP60 failed to bind. Neither CRT nor HSP60 bound to the control peptide 65–79*0402 affinity column. Thus, the retention of CRT on SE-positive peptide affinity columns represents direct interaction.

CRT is expressed both intracellularly and on the cell surface. To determine whether the SE can interact with surface CRT, cell surface proteins were biotinylated *in vivo* in intact cells, purified on a monomeric avidin column, and then subjected to peptide affinity chromatography. As can be seen (Fig. 1*D*), cell surface CRT interacted specifically with the SE-positive peptide 65–79*0404, but failed to bind to the SE-negative peptide 65–79*0402.

To determine whether the native DR molecule interacts with native surface CRT, cell-binding assays were performed between

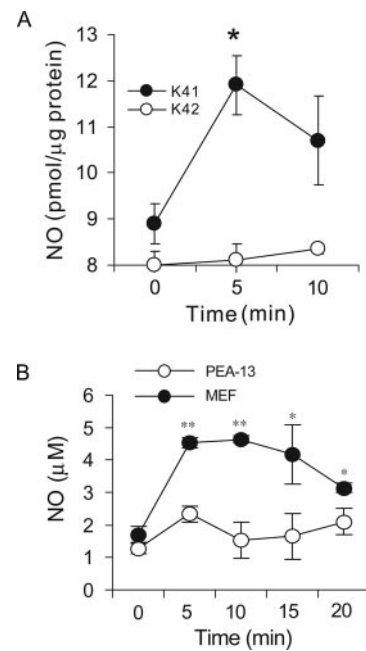


FIGURE 6. CRT is essential for SE-triggered signaling. *A*, MEF derived from wild-type mice (K41, ●) or *crt*^{-/-} mice (K42, ○) were incubated with Sepharose-immobilized 65–79*0401 peptide as above and NO levels were determined at different time points. *, $p < 0.005$. *B*, Wild-type (●) or CD91-deficient (PEA-13, ○) MEF were incubated with Sepharose-immobilized 65–79*0401 peptide as above and NO levels were determined at different time points. *, $p < 0.02$; **, $p < 0.005$.

M1 cells, which constitutively express CRT on their surface, and L cell transfectants expressing SE-positive or SE-negative surface HLA-DR molecules (Fig. 2). As can be seen, L565.5 transfectants (expressing on their surface the SE-positive DR molecule encoded by *DRA1*0101/DRB1*0401*) had a more robust interaction with M1 cells, compared with transfectants L514.3 (*DRA1*0101/DRB1*0402*) or L259.3 (*DRA1*0101/DRB1*0403*), which express SE-negative DR molecules on their surfaces. Anti-CRT Abs inhibited the interaction, confirming the identity of the SE-binding molecule as cell surface CRT (Fig. 2). The incomplete inhibitory effect suggests that the Abs produced only partial steric hindrance, although the possibility that cell surface molecules besides CRT may contribute to the binding deserves further consideration.

To better characterize the interaction between the SE and CRT and to determine the fine molecular specificity of this interaction, we used a SPR technique. rCRT was immobilized on a biosensor chip and different synthetic peptides were injected in the analyte. As can be seen (Fig. 3*A*), SE-positive peptides 65–79*0401 and 65–79*0404 bound to CRT in biologically significant affinities ($K_D = 10.8 \times 10^{-6}$ M and 11×10^{-6} M, respectively), while the SE-negative peptide 65–79*0402 did not show any binding. A truncated protein containing the CRT N domain only did not bind SE-expressing peptides, suggesting that the SE binding site is outside the CRT N domain.

The specificity of SE/CRT binding was further corroborated by a TR-FRET-binding assay. Binding of 15-mer peptides to CRT was determined by labeling biotinylated peptides with Cy5-streptavidin as the acceptor unit. On the donor side, we used a CRT-GST fusion protein and a europium cryptate-labeled anti-GST Ab (Fig. 3*B*, upper panel). TR-FRET assays showed that CRT binding of the SE-positive peptide 65–79*0404 was much more robust than the SE-negative peptide 65–79*0402 ($p < 0.0001$, Fig. 3*B*, lower panel). Using a panel of 5-mer peptides

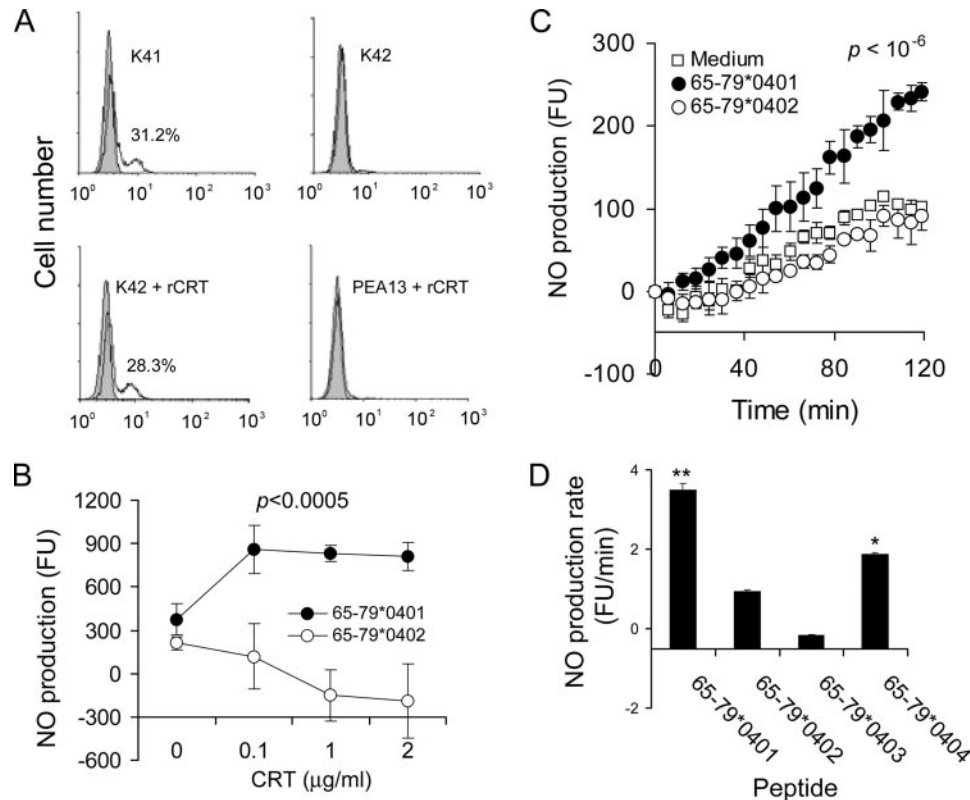


FIGURE 7. Exogenously added rCRT binds to the cell surface and restores SE-triggered signaling in *crt*^{-/-} cells. **A**, MEF were cultured for 1 h with or without 2 µg/ml rCRT and analyzed by flow cytometry. Shaded histograms represent cells stained with second-stage Abs (goat anti-rabbit IgG-FITC) only. White histograms represent cells stained with both first (rabbit anti-CRT) and second-stage Abs. The numbers represent the percentage of positively stained cells. **B**, *crt*^{-/-} MEF were incubated overnight with different concentrations of recombinant CRT, then washed and stimulated with 100 µg/ml either SE-positive peptide 65-79*0401 (●) or SE-negative peptide 65-79*0402 (○). NO production was determined at the end of 420 min of incubation. The *p* value, which pertains to the difference between the two entire curves, was calculated using a paired Student *t* test analysis. **C**, *crt*^{-/-} MEF were incubated overnight with 1 µg/ml rCRT, then washed and incubated either with 100 µg/ml SE-positive peptide 65-79*0401 (●), 100 µg/ml SE-negative peptide 65-79*0402 (○), or medium only (□). NO production was determined at different time points. The *p* value, which pertains to the difference between the two entire curves, was calculated using a paired Student *t* test analysis. **D**, *crt*^{-/-} MEF cells were incubated overnight with rCRT (1 µg/ml), then washed and stimulated with 100 µg/ml SE-positive (65-79*0401 or 65-79*0404) or SE-negative (65-79*0402 or 65-79*0403) peptides. NO production rates (fluorescence units/min) during the 200–420 min time interval were measured as previously described (8).

containing single amino acid substitutions, we have previously identified a consensus amino acid motif of Q/R-K/R-x-x-A that is necessary and sufficient for triggering SE-dependent signaling (9). Consistent with those findings, we demonstrate here that 5-mer peptides expressing the Q/R-K/R-x-x-A motif bound specifically to CRT in SPR assays (Fig. 3C). Thus, the same motif is required both for interaction and signal transduction.

To determine whether CRT plays a role in SE-triggered signal transduction, we first examined the effect of blocking Abs. Both anti-CRT Abs and Abs against the CRT surface-binding molecule CD91 (17) completely blocked SE-triggered signaling (Fig. 4A). Additionally, CRT antisense oligonucleotides suppressed CRT surface expression (Fig. 4B), inhibited SE-triggered NO production (Fig. 4C), and blocked the pro-oxidative effect of the SE ligand (Fig. 4A). Likewise, CRT-targeted siRNA oligonucleotides effectively silenced CRT mRNA expression (Fig. 5A) and inhibited SE-triggered signaling (Fig. 5B). Additionally, SE-positive peptides triggered NO signaling in a wild-type MEF, but no response was seen in MEF from a *crt*^{-/-} (Fig. 6A) or a CD91-deficient mouse (Fig. 6B).

A recent study has demonstrated that exogenous rCRT added to culture medium attached to the surface of CRT-deficient cells and restored CRT-dependent immunogenic signaling events (18). To examine whether soluble CRT could restore SE signaling in CRT-

deficient cells, we investigated SE-triggered signaling events in *crt*^{-/-} MEF, which had been preincubated with the recombinant protein. Adding soluble CRT restored surface expression of CRT to a level comparable to that observed in the wild-type MEF (Fig. 7A). In contrast, CD91-deficient MEF (PEA-13) failed to bind soluble CRT on their surface, consistent with CD91 proposed role as CRT receptor (17). Importantly, soluble CRT restored the responsiveness of *crt*^{-/-} MEF to SE-triggered signaling (Fig. 7, B–D), while it had no such effect on CD91-negative cells (data not shown). Thus, taken collectively, our data indicate that CRT is the cell surface protein that interacts with the SE and transduces its signaling.

Discussion

In this study, we demonstrate that cell surface CRT plays a critical role in SE-triggered signaling. The results reported here support four main conclusions: 1) SE-CRT interaction depends on a specific SE motif; 2) CRT is essential for SE-triggered signaling; 3) CD91 is necessary for CRT-mediated SE-triggered signal transduction; 4) soluble CRT can restore SE signaling in CRT-deficient cells.

We have previously identified a consensus Q/R-K/R-x-x-A motif, which is required for SE-triggered signaling (9). In the present study, we provide evidence that the same motif is required for

SE-CRT interaction. SE-positive, but not SE-negative, peptides, interacted with rCRT in SPR assays in biologically significant affinities. The calculated binding affinities between CRT and SE-expressing 15-mer peptides ($K_D = \sim 11 \times 10^{-6}$ M) were at the same range as binding affinities previously documented for many other immune system receptors, such as HLA class I molecules/NK receptors, class I MHC/TCR, CD2/CD58, as well as CD80/CD28 (reviewed in Ref. 19).

TR-FRET-based binding studies with 15-mer peptides that differ by only 3-aa residues corroborated SE-CRT-binding specificity (Fig. 3B). Furthermore, experiments with soluble CRT demonstrated that even a single amino acid difference (e.g., DR β residue 74 alanine vs glutamic acid in alleles *0404 and *0403, respectively) was sufficient to prevent CRT-dependent SE-triggered signaling (Fig. 7D). Similarly, experiments with 5-mer peptides (Fig. 3C) demonstrated that the SE motif is necessary for the interaction in a cell-free system, in agreement with our previous signal transduction finding in intact cells (9). It is noteworthy that population-based immunogenetic analyses have shown that the Q/R-K/R-x-x-A sequence in residues 70–74 of the DR β -chain correlate best with RA (20). Thus, the data shown here are consistent both with our previous findings and epidemiological analyses.

SPR-binding studies between 5-mer peptides and CRT (Fig. 3C) showed that peptide RRRAA produced a substantially higher RU reading compared with peptide QKRAA. The sequence RRRAA is the SE motif encoded by *DRB1**1001, a relatively rare allele that according to some studies is associated with more severe RA (21). It is therefore tempting to speculate that the higher RU values observed with peptide RRRAA is biologically meaningful. It should be cautioned, however, that RU values do not correlate well with affinities, as exemplified in Fig. 3A. Although substantial RU differences were found between SE-positive 15-mer peptides 65–79*0401 and 65–79*0404, the K_D values of these two peptides were very similar.

In addition to characterizing its role as a specific SE-binding molecule, we demonstrate here that CRT is essential for SE-triggered signaling. Anti-CRT Abs, *crt* gene disruption or mRNA silencing, were all found to interfere with SE-triggered signaling, indicating that CRT plays a critical role in SE-induced signaling activation. Because CRT lacks a transmembrane domain, it has been previously proposed that CD91 is serving as a CRT receptor (17). Consistent with a recent report (18), we demonstrated here that adding soluble CRT to *crt*^{-/-} MEF restored signaling. Furthermore, we also show that SE-triggered signaling depends on the expression of both CD91 (Figs. 4 and 6) and CRT (Figs. 4–6) and soluble CRT does not attach to the surface CD91-deficient cells. Thus, taken collectively, our findings suggest that CD91 may be functioning as a coreceptor for the SE by serving as a surface attachment molecule for CRT. This idea requires further experimental exploration.

CRT is a ubiquitous multifunctional calcium-binding protein. Although originally characterized as an ER molecular chaperone, more recently it has been shown to be present on the surface of many cell types and has been implicated in signal transduction events associated with innate immunity, cell adhesion, angiogenesis, and apoptosis (reviewed in Ref. 22). Cell surface CRT plays a pivotal role in the removal of apoptotic cells and, depending on the cosignaling context, ligation of CRT can lead to activation of either pro- or anti-inflammatory pathways (23). Impairments, which upset this multifactorial balance, could conceivably result in autoimmunity (24). Indeed, CRT has long been considered potential culprit in autoimmune diseases, including RA (13). Two previous reports proposed a direct role for CRT in RA pathogenesis (25, 26). Verreck et al. (25) immunoprecipitated HLA-DR/peptide

complexes from DR4Dw4(*DRB1**0401)/DRw53-positive EBV-transformed B cells and eluted from those complexes a 15-mer peptide corresponding to amino acids 278–292 of human CRT. Max et al. (26) eluted from similar immunoprecipitates a 16-mer peptide corresponding to the same region of the protein. Both groups hypothesized that the origin of those peptides was from the HLA-DR peptide-binding groove. However, in light of the data presented here, it is equally plausible that rather than representing bona fide antigenic groove peptides, those peptides could have been fragments of SE-bound CRT.

Consistent with our previous studies showing that the SE acts as a pro-oxidative signal-triggering ligand (9), CRT has long been known to play important roles in cellular stress responses in the innate immune system (27–33). Binding of C1q to neuronal cell surface CRT triggers increased levels of cellular reactive oxygen species (29). In neutrophils, CRT engagement by C1q leads to production of superoxide (30). Similarly, in monocytes (31) and neutrophils (32), cell surface CRT binds the antibacterial peptide L5 and transduces superoxide-dependent bactericidal signaling. In addition, in monocytes, cell surface CRT binds the neutrophil secretory protein azurocidin, which results in increased production of IL-6 (33). Thus, cell surface CRT is an important innate immune system receptor.

The results presented here suggest that by binding the SE ligand, CRT may function as a bridge, which allows an adaptive immune system molecule to aberrantly activate an innate system signal transduction pathway. We believe these data could help explaining some of the enigmas surrounding RA-SE associations (reviewed in 34). For example, an adaptive immune mechanism is difficult to reconcile with the fact that although presentation of antigenic peptides to CD4⁺ T cells is the best known function of class II MHC molecules, there is no conclusive evidence to indicate that Ag presentation is the mechanism underlying SE-RA association.

Additionally, SE disease association is not exclusive for RA, as several other human diseases have been shown to be significantly more common in individuals carrying SE-encoding *DRB1* alleles (35–39). SE-positive *DRB1* alleles can also aggravate collagen-induced arthritis (40, 41) and experimental autoimmune encephalomyelitis (42), and trigger spontaneous diabetes (43) in transgenic mice. Endogenous SE-encoding class II MHC genes are associated with spontaneous arthritis in dogs (44) and a multitude of induced or spontaneous autoimmune diseases in SJL mice (45–47). These pathogenically distinct models involve immune responses to many unrelated target Ags. Attributing the effect of the SE in all these conditions to Ag presentation is inconsistent with the structural stringency of the SE motif on the one hand, and the strict specificity in which antigenic epitope are being recognized, on the other.

Furthermore, several studies have shown that advancing age is a strong risk factor both in RA (48) and in several spontaneous SE-associated autoimmune diseases in mice (43, 46). Such aging-associated susceptibility is unlikely to be due to improved presentation of specific Ags, because adaptive immune responses are expected to decline with age. Finally, a strictly adaptive immunity based mechanism is inconsistent with the positive correlations observed between the number of copies of SE-encoding alleles and RA severity (49) and penetrance (50).

The mechanism proposed here provides plausible explanations to these inconsistencies; it could better explain why SE associations lack Ag, species, or disease specificity. A signal transduction-based paradigm is also more consistent with the dose-dependent nature of SE associations. Similarly, it is conceivable that due to its pro-oxidative effect, the SE accelerates an aging-associated epigenetic drift or increases the frequency of stochastic events, thereby

continuously increasing the risk of triggering disease-initiating aberrations (reviewed in Ref. 34).

It should be clarified, however, that the mechanism proposed above does not rule out the involvement of groove peptides in RA. It is possible that while class II MHC-restricted Ag presentation determines the specificity of the immune response, SE-triggered innate signaling determines its intensity, or its proinflammatory polarization. It is also possible that certain groove peptides may have a stabilizing effect on SE-expressing class II molecules, thereby allowing a more efficient interaction with CRT.

Activation of innate immune receptors by adaptive immune system ligands is not without precedence. Ligands encoded by class I MHC superfamily genes interact with a diverse repertoire of activating or inhibitory innate immune system receptors. For example, classical class I MHC molecules have been shown to bind to KIR and modulate NK cytolytic activity (2). Similarly, the human non-classical class I MHC molecule HLA-E interacts with NKG2/CD94 and alters the effector function of NK cells (4) and non Ag-presenting class I MHC-like molecules bind to NKG2D receptors and activate antitumor cytolytic responses (3). Similar to the SE, class I MHC ligand-triggered activation of innate immune signaling has been proposed to play a role in autoimmunity (51). Different from class I ligand-mediated effect, however, SE signaling is allele restricted.

Our data indicate that, similar to the engagement of NK receptors by class I MHC ligands, the interaction between the SE and CRT can take place in *trans* (i.e., between two opposite cells). Whether *in-cis* interactions (5, 6) are also possible is presently unknown. It is also unclear whether other cell surface receptors can affect the intensity of SE-CRT interaction or its functional consequences. As mentioned above, depending on the cosignaling context, CRT ligation can lead to activation of either pro- or anti-inflammatory pathways. We propose that investigating those signal modulating pathways in RA could provide important insights into the role of the SE-CRT axis in the pathogenesis of this disease.

Acknowledgments

We thank Drs. Emanuel Kamberov and Qiang Jia for expert technical assistance. Special thanks to Dr. Robert Karr for his gift of L cell transfectants and to Dr. Marek Michalak for his advice and encouragements and for providing plasmids and cell lines.

Disclosures

J. Holoshitz and S. Ling are coinventors of a related technology owned by the Regents of the University of Michigan.

References

- Gregersen, P. K., J. Silver, and R. J. Winchester. 1987. The shared epitope hypothesis: an approach to understanding the molecular genetics of susceptibility to rheumatoid arthritis. *Arthritis Rheum.* 30: 1205–1213.
- Radaev, S., and P. D. Sun. 2003. Structure and function of natural killer cell surface receptors. *Annu. Rev. Biophys. Biomol. Struct.* 32: 93–114.
- Bauer, S., V. Groh, J. Wu, A. Steinle, J. H. Phillips, L. L. Lanier, and T. Spies. 1999. Activation of NK cells and T cells by NKG2D, a receptor for stress-inducible MICA. *Science* 285: 727–729.
- Braud, V. M., D. S. Allan, C. A. O'Callaghan, K. Soderstrom, A. D'Andrea, G. S. Ogg, S. Lazetic, N. T. Young, J. I. Bell, J. H. Phillips, et al. 1998. HLA-E binds to natural killer cell receptors CD94/NKG2A, B and C. *Nature* 391: 795–799.
- Bennett, M. J., J. A. Lebron, and P. J. Bjorkman. 2000. Crystal structure of the hereditary haemochromatosis protein HFE complexed with transferrin receptor. *Nature* 403: 46–53.
- Loconto, J., F. Papes, E. Chang, L. Stowers, E. P. Jones, T. Takada, A. Kumanovics, K. Fischer Lindahl, and C. Dulac. 2003. Functional expression of murine V2R pheromone receptor involves selective association with the M10 and M1 families of MHC class Ib molecules. *Cell* 112: 607–618.
- Brown, J. H., T. S. Jardetzky, J. C. Gorga, L. J. Stern, R. G. Strominger, and D. C. Wiley. 1993. Three-dimensional structure of the human class II histocompatibility antigen HLA-DR1. *Nature* 364: 33–39.
- Ling, S., A. Lai, O. Borschukova, P. Pumpens, and J. Holoshitz. 2006. Activation of nitric oxide signaling by the rheumatoid arthritis shared epitope. *Arthritis Rheum.* 54: 3423–3432.
- Ling, S., Z. Li, O. Borschukova, L. Xiao, P. Pumpens, and J. Holoshitz. 2007. The rheumatoid arthritis shared epitope increases cellular susceptibility to oxidative stress by antagonizing an adenosine-mediated anti-oxidative pathway. *Arthritis Res. Ther.* 9:R5.
- Gleimer, M., and P. Parham. 2003. Stress management: MHC class I and class I-like molecules as reporters of cellular stress. *Immunity* 19: 469–477.
- Vassilakos, A., M. Michalak, M. A. Lehrman, and D. B. Williams. 1998. Oligosaccharide binding characteristics of the molecular chaperones calnexin and calreticulin. *Biochemistry* 37: 3480–3490.
- Mesaeli, N., K. Nakamura, E. Zvaritch, P. Dickie, E. Dziak, K. H. Krause, M. Opas, D. H. MacLennan, and M. Michalak. 1999. Calreticulin is essential for cardiac development. *J. Cell Biol.* 144: 857–868.
- Eggleton, P., and D. H. Llewellyn. 1999. Pathophysiological roles of calreticulin in autoimmune disease. *Scand. J. Immunol.* 49: 466–473.
- Macht, L. M., C. J. Elson, J. R. Kirwan, J. S. Gaston, A. G. Lamont, J. M. Thompson, and S. J. Thompson. 2000. Relationship between disease severity and responses by blood mononuclear cells from patients with rheumatoid arthritis to human heat-shock protein 60. *Immunology* 99: 208–214.
- Fitzgerald, M., and D. Keast. 1994. Fab fragments from the monoclonal antibody ML30 bind to treated human myeloid leukemia cells. *FASEB J.* 8: 259–261.
- White, T. K., Q. Zhu, and M. L. Tanzer. 1995. Cell surface calreticulin is a putative mannoside lectin which triggers mouse melanoma cell spreading. *J. Biol. Chem.* 270: 15926–15929.
- Basu, S., R. J. Binder, T. Ramalingam, and P. Seivastava. 2001. CD91 is a common receptor for heat shock proteins gp96, HSP70 and calreticulin. *Immunity* 14: 303–313.
- Obeid, M., A. Tesniere, F. Ghiringhelli, G. M. Fimia, L. Apetoh, J. L. Perfettini, M. Castedo, G. Mignot, T. Panaretakis, N. Casares, et al. 2007. Calreticulin exposure dictates the immunogenicity of cancer cell death. *Nat. Med.* 13: 54–61.
- Vales-Gomez, M., H. Reyburn, and J. Strominger. 2000. Molecular analyses of the interactions between human NK receptors and their HLA ligands. *Hum. Immunol.* 61: 28–38.
- Ou, D., L. A. Mitchell, and A. J. Tingle. 1998. A new categorization of HLA DR alleles on a functional basis. *Hum. Immunol.* 59: 665–676.
- Ioannidis, J. P., K. Tarassi, I. A. Papadopoulos, P. V. Voulgari, K. A. Boki, C. A. Papasteriades, and A. A. Drosos. 2002. Shared epitopes and rheumatoid arthritis: disease associations in Greece and meta-analysis of Mediterranean European populations. *Semin. Arthritis Rheum.* 31: 361–370.
- Johnson, S., M. Michalak, M. Opas, and P. Eggleton. 2001. The ins and outs of calreticulin: from the ER lumen to the extracellular space. *Trends Cell Biol.* 11: 122–129.
- Henson, P. M., D. L. Bratton, and V. A. Fadok. 2001. The phosphatidylserine receptor: a crucial molecular switch? *Nat. Rev. Cell Biol.* 2: 627–633.
- Donnelly, S., W. Roake, S. Brown, P. Young, H. Naik, P. Wordsworth, D. A. Isenberg, K. B. Reid, and P. Eggleton. 2006. Impaired recognition of apoptotic neutrophils by the C1q/calreticulin and CD91 pathway in systemic lupus erythematosus. *Arthritis Rheum.* 54: 1543–1556.
- Verreck, F. A., D. Elferink, C. J. Vermeulen, R. Amons, F. Breedveld, R. R. de Vries, and F. Koning. 1995. DR4Dw4/DR53 molecules contain a peptide from the autoantigen calreticulin. *Tissue Antigens* 45: 270–275.
- Max, H., T. Halder, M. Kalbus, V. Gnaul, G. Jung, and H. Kalbacher. 1994. A 16mer peptide of the human autoantigen calreticulin is a most prominent HLA-DR4Dw4-associated self-peptide. *Hum. Immunol.* 41: 39–45.
- Jethmalani, S. M., and K. J. Henle. 1998. Calreticulin associates with stress proteins: implications for chaperone function during heat stress. *J. Cell. Biochem.* 69: 30–43.
- Gardai, S. J., Y. Q. Xiao, M. Dickinson, J. A. Nick, D. R. Voelker, K. E. Greene, and P. M. Henson. 2003. By binding SIRP α or calreticulin/CD91, lung collectins act as dual function surveillance molecules to suppress or enhance inflammation. *Cell* 115: 13–23.
- Luo, X., G. A. Weber, J. Zheng, H. E. Gendelman, and T. Ikezu. 2003. C1q-Crt induced oxidative neurotoxicity: relevance for the neuropathogenesis of Alzheimer's disease. *J. Neuroimmunol.* 135: 62–71.
- Tenner, A. J., and N. R. Cooper. 1982. Stimulation of a human polymorphonuclear leukocyte oxidative response by the C1q subunit of the first complement component. *J. Immunol.* 128: 2547–2552.
- Cho, J. H., K. J. Homma, S. Kanegasaki, and S. Natori. 2001. Activation of human monocyte cell line U937 via cell surface calreticulin. *Cell Stress Chaperones* 6: 148–152.
- Cho, J. H., K. J. Homma, S. Kanegasaki, and S. Natori. 1999. Activation of human neutrophils by a synthetic anti-microbial peptide, KLKLLLLLKLK-NH₂, via cell surface calreticulin. *Eur. J. Biochem.* 266: 878–885.
- Okuyama, Y., J. H. Cho, Y. Nakajima, K. Homma, K. Sekimizu, and S. Natori. 2004. Binding between azurocidin and calreticulin: its involvement in the activation of peripheral monocytes. *J. Biochem.* 135: 171–177.
- Holoshitz, J., and S. Ling. 2007. Nitric oxide signaling triggered by the rheumatoid arthritis shared epitope: a new paradigm for MHC-disease association? *Ann. New York Acad. Sci.* 110: 73–83.
- Doherty, D. G., P. T. Donaldson, J. A. Underhill, J. M. Farrant, A. Duthie, G. Mieli-Vergani, I. G. McFarlane, P. J. Johnson, A. L. Eddleston, A. P. Mowat, et al. 1994. Allelic sequence variation in the HLA class II genes and proteins in patients with autoimmune hepatitis. *Hepatology* 19: 609–615.

36. Dorak, M. T., H. K. Machulla, M. Hentschel, K. I. Mills, J. Langner, and A. K. Burnett. 1996. Influence of the major histocompatibility complex on age at onset of chronic lymphoid leukaemia. *Int. J. Cancer* 65: 134–139.
37. Tait, B. D., B. P. Drummond, M. D. Varney, and L. C. Harrison. 1995. HLA-DRB1*0401 is associated with susceptibility to insulin-dependent diabetes mellitus independently of the *DQB1* locus. *Eur. J. Immunogenet.* 22: 289–297.
38. Korendowych, E., J. Dixey, B. Cox, S. Jones, and N. McHugh. 2003. The influence of the HLA-DRB1 rheumatoid arthritis shared epitope on the clinical characteristics and radiological outcome of psoriatic arthritis. *J. Rheumatol.* 30: 96–101.
39. Weyand, C. M., N. N. Hunder, K. C. Hicok, G. G. Hunder, and J. J. Goronzy. 1994. HLA-DRB1 alleles in polymyalgia rheumatica, giant cell arteritis, and rheumatoid arthritis. *Arthritis Rheum.* 37: 514–520.
40. Rosloniec, E. F., D. D. Brand, L. K. Myers, K. B. Whittington, M. Gumanovskaya, D. M. Zaller, A. Woods, D. M. Altmann, J. M. Stuart, and A. H. Kang. 1997. An HLA-DR1 transgene confers susceptibility to collagen-induced arthritis elicited with human type II collagen. *J. Exp. Med.* 185: 1113–1122.
41. Andersson, E. C., B. E. Hansen, H. Jacobsen, L. S. Madsen, C. B. Andersen, J. Engberg, J. B. Rothbard, G. S. McDevitt, V. Malmström, R. Holmdahl, et al. 1998. Definition of MHC and T cell receptor contacts in the HLA-DR4-restricted immunodominant epitope in type II collagen and characterization of collagen-induced arthritis in HLA-DR4 and human CD4 transgenic mice. *Proc. Natl. Acad. Sci. USA* 95: 7574–7579.
42. Ito, K., H. J. Bian, M. Molina, J. Han, J. Magram, E. Saar, C. Belunis, D. R. Bolin, R. Arceo, R. Campbell, et al. 1996. HLA-DR4-IE chimeric class II transgenic, murine class II-deficient mice are susceptible to experimental allergic encephalomyelitis. *J. Exp. Med.* 183: 2635–2644.
43. Gebe, J. A., K. A. Unrath, B. A. Falk, K. Ito, L. Wen, T. L. Daniels, A. Lernmark, and G. T. Nepom. 2006. Age-dependent loss of tolerance to an immunodominant epitope of glutamic acid decarboxylase in diabetic-prone RIP-B7/DR4 mice. *Clin. Immunol.* 121: 294–304.
44. Ollier, W. E., L. J. Kennedy, W. Thomson, A. N. Barnes, S. C. Bell, D. Bennett, J. M. Angles, J. F. Innes, and S. D. Carter. 2001. Dog MHC alleles containing the human RA shared epitope confer susceptibility to canine rheumatoid arthritis. *Immunogenetics* 53: 669–673.
45. Mengle-Gaw, L., and H. O. McDevitt. 1985. Predicted protein sequence of the murine I-E- β^s polypeptide chain from cDNA and genomic clones. *Proc. Natl. Acad. Sci. USA* 82: 2910–2914.
46. Weller, A. H., S. A. Magliato, K. P. Bell, and N. L. Rosenberg. 1997. Spontaneous myopathy in the SJL/J mouse: pathology and strength loss. *Muscle Nerve.* 20: 72–82.
47. Ding, M., M. Zhang, J. L. Wong, N. E. Rogers, L. J. Ignarro, and R. R. Voskuhl. 1998. Antisense knockdown of inducible nitric oxide synthase inhibits induction of experimental autoimmune encephalomyelitis in SJL/J mice. *J. Immunol.* 160: 2560–2564.
48. Goronzy, J. J., and C. M. Weyand. 2005. Rheumatoid arthritis. *Immunol. Rev.* 204: 55–73.
49. Gonzalez-Gay, M. A., C. Garcia-Porrua, and A. H. Hajeer. 2002. Influence of human leukocyte antigen-DRB1 on the susceptibility and severity of rheumatoid arthritis. *Semin. Arthritis Rheum.* 31: 355–360.
50. Jawaheer, D., W. Thomson, A. J. MacGregor, D. Carthy, J. Davidson, P. A. Dyer, A. J. Silman, and W. E. R. Ollier. 1994. “Homozygosity” for the HLA-DR shared epitope contributes the highest risk for rheumatoid arthritis concordance in identical twins. *Arthritis Rheum.* 37: 681–686.
51. Rajagopalan, S., and E. O. Long. 2005. Understanding how combinations of HLA and *KIR* genes influence disease. *J. Exp. Med.* 201: 1025–1029.